Moroccan Journal of Chemistry
ISSN : 2351-812X

Mor. J. Chem., 2023, Volume 11, Issue 2, Page 566-578
https://revues.imist.ma/index.php/morjchem

Structure – properties study of sodium bismuth borate glasses

Abid M. [1, 2 *], El-Hars F. [3 **], Belfaquir M. [2], Laourayed M. [4], Bakkali S. [5], Hafid M. [3], Taibi M. [6]

[1] Laboratory of Sciences and Pedagogical Innovation, Regional Center for Education and Training Trades, Rabat-Salé-Kenitra Region, 10000 Rabat, Morocco,
[2] Advanced Materials and Process Engineering Laboratory, Faculty of Sciences, Ibn Tofaıl University, BP 133, 14000 Kénitra, Morocco,
[3] Laboratory of Materials and Subatomic Physic, Faculty of Sciences, Ibn Tofaıl University, BP 133, 14000 Kénitra, Morocco,
[4] Laboratory of Materials, Nanotechnology, and Environment, Faculty of Sciences, Mohammed V University, 10000 Rabat, Morocco,
[5] Laboratory of Analytical and Molecular Chemistry, Polydisciplinary Faculty of Safi, Cadi Ayyad University, Safi, Morocco,
[6] Laboratory of Physicochemistry of Inorganic and Organic Materials, ENS Takaddoum, Mohammed V University, 10000 Rabat, Morocco.
**Corresponding author, Email address: abid.mohammed@uit.ac.ma*
***Corresponding author, Email address: elhars.fouad.mstr@gmail.com*

***Received** 07 April 2022, **Revised** 23 Feb 2023, **Accepted** 28 March 2023*

Citation: Abid M., El-Hars F., Belfaquir M., Laourayed M., Bakkali S., Hafid M., Taibi M. (2023) Structure – properties study of sodium bismuth borate glasses, Mor. J. Chem., 11(2),566-578.
*Doi:*https://doi.org/10.48317/IMIST.PRSM/morjchem-v11i1.31823

Abstract: Sodium bismuth borate glasses with composition (100–x)(0.785B_2O_3–0.215Bi_2O_3)–xNa_2O where x=0, 2, 4, 6 and 8 mol%, were prepared by standard synthesized melt–quenching method. The amorphous and vitreous nature of these samples was confirmed by X–ray diffraction (XRD) and differential scanning calorimetry (DSC) analysis. The density of the samples was measured using Archimedes principle and the molar volumes were determined from the density data. The spectroscopic properties of glass samples were studied using Fourier Transform Infrared Spectrometer (FTIR) and Raman spectroscopic techniques. The density of the samples was found to vary non–linearly with the Na_2O content, however, a slight variation of the glass transition temperature was observed. The addition of Na_2O in 78.5B_2O_3–21.5Bi_2O_3 glass causes changes in the features of the FTIR and Raman spectra. Both types of IR and Raman spectroscopic revealed that the network structure of the studied glasses is mainly based on BO_3 and BO_4 units, and bismuth exists as BiO_3 pyramidal and BiO_6 octahedral units.

Keywords: Bismuth borate glasses, Density, Molar volume, Structure, DSC, FTIR, Raman

1. Introduction

Among various oxide glasses, B_2O_3 can form glasses either alone or when mixed with considerable quantities of non–glass–forming oxides whereas Bi_2O_3 is conditional glass former. Growing attention has been given to borate glasses because they generally offer some unique

physical properties better than other glasses, such as low melting point, high transparency and good thermal stability (Bengisu *et al.*, 2016), (Minakova *et al.*, 2008). Recently, systematic studies have been conducted on the effect of bismuth ions (Bi^{3+}) on the structure and properties of bismuth–borate glasses (Bajaj et *al.*, 2009), (Sanghi et *al.*, 2011), (Doweidar, 2014). It was suggested that the addition of Bi_2O_3 to the borate glasses improves the chemical durability and thermal stability of the samples (Shaaban et *al.*, 2008). Bismuth borates have been stated to form transparent glasses over a particularly wide range of Bi_2O_3 contents, from 20 to 85 mol% (Bajaj et *al.*, 2009), in which Bi_2O_3 converts symmetrical BO_3 triangles into BO_4 tetrahedra until certain Bi_2O_3 content. Beyond this concentration, the asymmetric BO_3 triangles, which contain non–bridging oxygen ions (NBO), are formed at the expense of BO_4 tetrahedra. These processes induce to the appearance of maximum value of the fraction of four–coordinated boron. It is expected that Bi_2O_3 enters the borate matrix in the form of trigonal BiO_3 trigonal pyramids (with a Bi apex) and BiO_6 octahedra or in the form of BiO_3 or BiO_6 units. The type of structural units depends mainly on the glass and its composition. Alkali borate glass systems are good candidates for ion conduction and suitable for the fabrication of solid–state batteries. Borate glasses with heavy metal ions such as Bi, Pb etc. exhibit good nonlinear optical properties (Rajyasree and Krishna Rao, 2011). In addition, it has been reported that the addition of Na_2O in bio-glass could be an important component in achieving an optimal combination of bioactivity and wettability (Bouhazma *et al.*, 2015). In the light of the above, the aim of the present work is to prepare and study the influence of NaO_2 addition on thermal and structural properties in the system $(100–x)(0.785B_2O_3–0.215Bi_2O_3)–xNa_2O$ (x=0–8 mol %) .

2. 2. Methodology

2.1 Sodium bismuth borate glasses preparation

The following sodium bismuth borate glass samples belonging $(100–x)(0.785B_2O_3–0.215Bi_2O_3)–xNa_2O$ (x=0–8 mol %), were prepared by melt–quenching method, from analytical pure reagent-grade of sodium carbonate (Na_2CO_3), bismuth oxide (Bi_2O_3) and boric acid (H_3BO_3) according to the reaction scheme (**Eqn. 1**):

$$xNa_2CO_3 + yBi_2O_3 + 2zH_3BO_3 \rightarrow [xNa_2O, yBi_2O_3, zB_2O_3] + 3zH_2O\nearrow + xCO_2\nearrow \qquad \textbf{Eqn. 1}$$

where x, y and z are the mole percent of Na_2O, Bi_2O_3 and B_2O_3 respectively.

The starting materials were mixed and ground firstly in an agate mortar and preheated in alumina crucible at 120°C overnight. To prevent product volatility, the temperature was then progressively increased to 1100°C and held constant at this value for 2h until homogeneous mixture was obtained. The batch was, finally, quenched at room temperature under air atmosphere to produce vitreous samples.

2.2 Sodium bismuth borate glasses characterization

2.4.1. X-ray diffraction

X–ray diffractograms of the powdered samples were recorded at room temperature using a Siemens D5000 diffractometer with Cu_K radiation (λ = 1.5418 Å) in the 2θ ranges of 10°–60° at a scanning rate of 2° per minute.

2.4.2. *Density, molar volume and oxygen packing density*

Density measurements were carried out at room temperature, using Archimedes' method with diethyl orthophthalate as the immersion fluid. The relative error in these measurements was about ±0.02 $g.cm^{-3}$. The molar volume V_m was calculated from the molecular weight M and density ρ of the glass according to the **Eqn. 2**. The absolute uncertainty is ±0.1 $cm^3.mol^{-1}$:

$$V_m = M/\rho; \qquad \textbf{Eqn. 2}$$

Also, the oxygen packing density (OPD) is calculated from the molecular weight M and density data ρ using the **Eqn. 3** (Ersundu *et al.*, 2011).

$$OPD = 1000\times C\times (\rho/M); \qquad \textbf{Eqn. 3}$$

where C is the number of oxygen atoms per each composition.

2.4.3. *Thermal study*

The XRD analysis was used to confirm the amorphous nature of the glasses. Differential scanning calorimetry of powder samples was made at a heating rate of 10 K/min using the DSC–SETARAM type apparatus 121 to determine the glass transition temperature (T_g); the estimated error is ±4°C.

2.4.4. *Fourier transform infrared spectroscopy*

The structural properties of the glasses were assessed using Fourier Transform Infrared (FTIR) Spectroscopy, in transmission mode. The measurements were made on glass powders dispersed in KBr pellets (3 wt%). The infrared spectra of the powder glass samples were recorded at room temperature in the range 400–1400 cm^{-1} using a FTIR Perkin-Elmer spectrometer.

2.4.5. *Raman spectroscopy*

Raman spectra were obtained in the range from 140 to 1400 cm^{-1} with a resolution of 2 cm^{-1} with a dispersive confocal Raman microscope (Renishaw inVia) using the 514 nm laser excitation line. The sample spot size of the Raman microscope is about 0.5 μm in diameter.

3. Results and discussion

Nominal compositions, density, molar volume, oxygen packing density, glass transition temperature and molar ratio of oxygen to boron for all the samples are listed in **Table 1**.

Table 1. Physical parameters of the $(100–x)(0.785B_2O_3–0.215Bi_2O_3)–xNa_2O$ glasses where $0\leq x \leq 8$ mol %

Parameters	Glass composition				
	x=0	**x=2**	**x=4**	**x=6**	**x=8**
Average molecular weight (g/mol)	154.83	153.09	150.96	149.22	147.48
Density ρ (g/cm^3)	4.62	4.53	4.45	4.37	4.29
Molar volume V_m (cm^3/mol)	33.49	33.94	34.33	34.73	35.15
Oxygen packing density (mol/L)	89.52	87.58	86.08	84.34	82.61
Glass transition temperature T_g (°C)	346	340	338	331	328
Crystallization temperature T_x (°C)	402	389	381	367	361
Thermal stability $T_x - T_g$	56	49	43	36	33
Ratio O/B	1.91	1.92	1.94	1.95	1.97

3.1. X-ray diffraction

As shown in **Figure 1**, the X–ray diffraction (XRD) patterns of typical glass sample, with nominal composition of $76.9B_2O_3$–$21.1Bi_2O_3$–$2Na_2O$ exhibits a broad diffuse scattering at different angles instead of crystalline peaks (Chourti *et al.*, 2020), confirming a long-range structural disorder characteristic of amorphous matrix (Abid *et al.*, 2019).

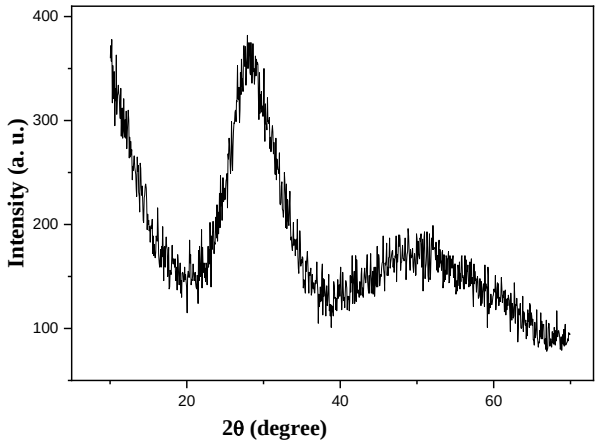

Figure 1. X–ray diffraction patterns for typical glass $76.9B_2O_3$–$21.1Bi_2O_3$–$2Na_2O$

3.2. Density, molar volume and oxygen packing density

The values of density (ρ), molar volume (V_m) and oxygen packing density (O) of each sample are listed in **Table 1** and are graphically presented in versus content of Na_2O in **Figure 2 & 3** respectively. As shown in **Figure 2**, the density ρ decreases linearly when Na_2O concentration increases in $(100–x)(0.785B_2O_3–0.215Bi_2O_3)–xNa_2O$ glasses from $4.62g.cm^{-3}$ for x_{Na2O}=0 mol% to $4.29g.cm^{-3}$ for 8 mol% of Na_2O. This result could be explained by considering the substitution of $0.785B_2O_3–0.215Bi_2O_3$ having high molecular mass $M=154.83g.mol^{-1}$, with Na_2O having a lower molecular mass $M_{Na2O}=61.98g.mol^{-1}$, the net molecular weight will decrease, thus, resulting in a decrease in density (El-Hezzat *et al.*, 2021), (Alaoui *et al.*, 2021). The obtained results show that both the molar volume (V_m) and the oxygen packing density (OPD) of the present glasses decrease with an increase of Na_2O content. The above results indicate the decrease in the tightness of the glass structure with the increase in the Na_2O content.

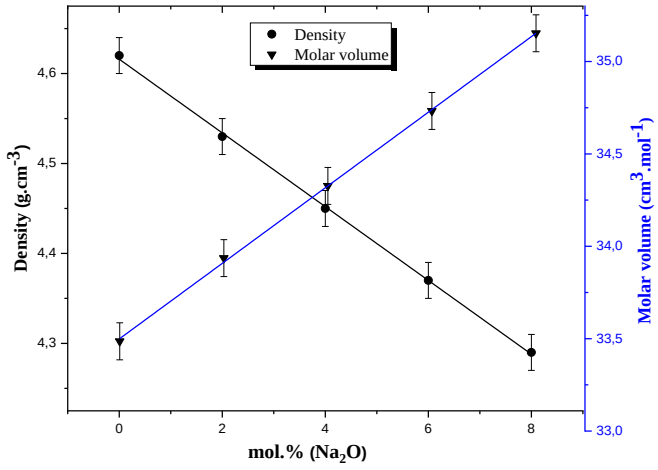

Figure 2. Composition dependence of density and molar volume of $(100–x)(0.785B_2O_3–0.215Bi_2O_3)–xNa_2O$ glasses

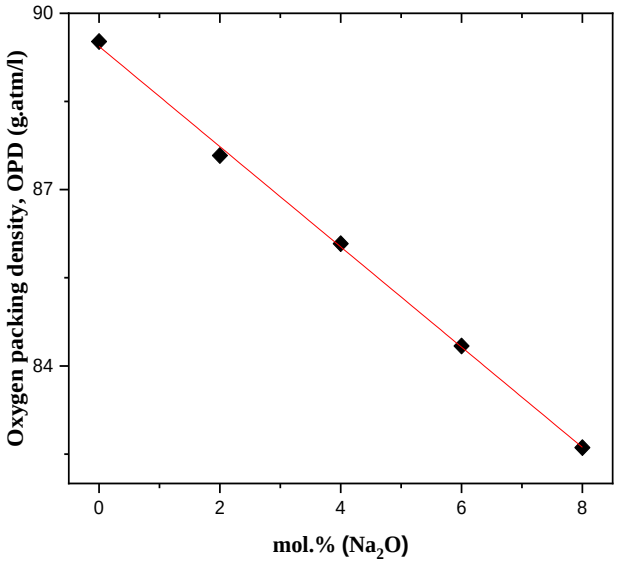

Figure 3. Composition dependence of oxygen packing density (OPD) of (100–x)(0.785B_2O_3–0.215Bi_2O_3)–xNa_2O glasses

3.3. Thermal analysis DSC

In Figure 4, a typical DSC curve of chosen glass composition of 76.9B_2O_3–21.1Bi_2O_3–2Na_2O is represented. The extracted data of onset glass transition temperature (T_g) and the onset crystallization temperature (T_x) are presented in **Table 1**. The variation of glass transition temperature T_g with the glass composition is shown in **Figure 5**. It can be observed that T_g values of the glasses decrease with Na_2O content. It is obvious that alkali metal oxide play the role of network modifier in silicate, phosphate and borate glasses and non–bridging oxygen increases with an increase in A_2O (A=Na, Li, K,..) in these glasses (Jabraoui *et al.*, 2016), (Suzuya *et al.*, 1998), (Padmaja and Kistaiah, 2009), which is confirmed in the studied glasses by the increasing of O/B ratio as shown in **Table 1**. It is widely known that the bond between the sodium atom and oxygen is ionic and is in general weaker than a covalent bond. Hence, T_g decreases with the increase of sodium oxide Na_2O content.

Table 1 summarizes the (T_x–T_g) values. It is known that (T_x–T_g) value is a good indicative of the thermal stability of glasses. As it can be seen from the **Table 1**, the glass samples without or with a low content of Na_2O, have a high value of (T_x – T_g), which reveals their large thermal stability against crystallization. Therefore, these samples have glass–forming ability.

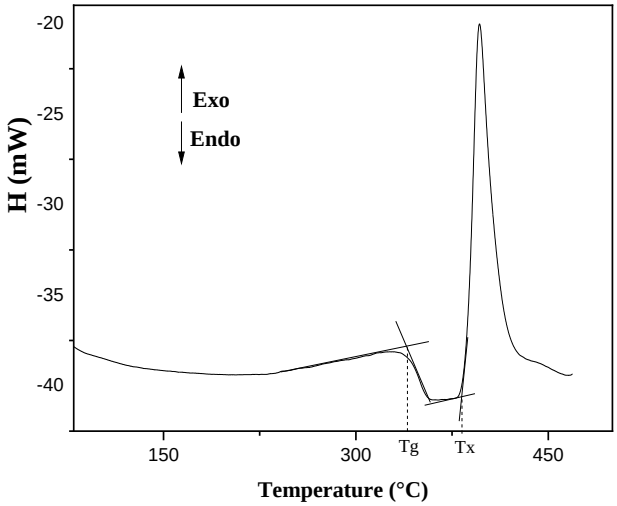

Figure 4. DSC curve of glass with composition 76.9B_2O_3–21.1Bi_2O_3 – 2Na_2O

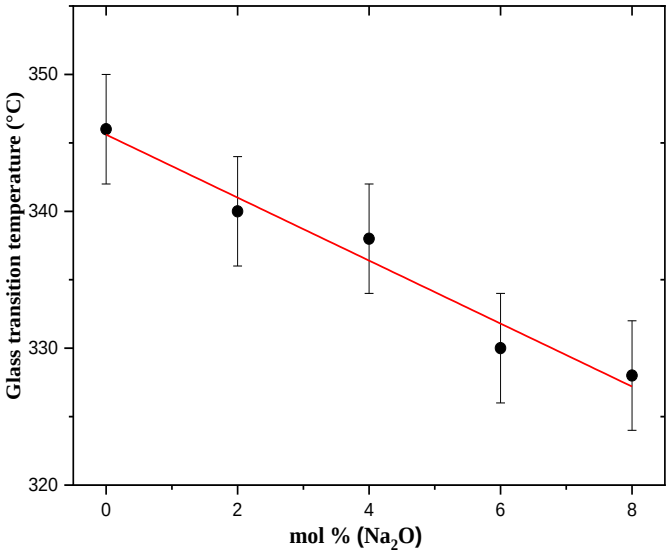

Figure 5. Composition dependence of glass transition temperature of (100–x)(0.785B_2O_3–0.215Bi_2O_3)–xNa_2O glasses

3.4. Structural study

3.4.1. Infrared spectroscopy

The infrared transmission spectra of (100–x)(0.785B_2O_3–0.215Bi_2O_3)–xNa_2O (0≤ x≤ 8mol.%) selected glasses are recorded at room temperature in the frequency range from 400 to1400 cm^{-1} as shown in **Figure 6**. The observed bands along with their vibrational assignments of samples are listed in **Table 2.** The obtained broad bands may confirm the amorphous nature of the studied glass samples and are agreement with XRD. Starting with the Na_2O−free glass 78.5B_2O_3–21.5Bi_2O_3 (x=0) spectrum, we notice the presence of the stretching vibrations of Bi–O bonds in a strongly distorted BiO_6 octahedral units at ~450 cm^{-1} (Dimitrov *et al.*, 1994), (Iordanova *et al.*, 1996), (Shaim *et al.*, 2002). The narrow and strong absorption band centered at ~710 cm^{-1} has been assigned to the B–O–B bending vibrations in BO_3 pyramidal units (Shaim *et al.*, 2002), (Sharma *et al.*, 2006), (Shaaban *et al.*, 2008) over which can be superposed the O_3B–O–BO_3 bending vibrations (Kamitsos *et al.*, 1987), (Motka *et al.*, 2002). The weaker shoulder band at ~900 cm^{-1} arises from symmetric stretching vibrations of Bi–O bonds in pyramidal BiO_3 units (Fuxi, 1991), possibly overlapped with stretching vibrations of B–O bonds in the BO_4 units of di-borate groups (Bhogi *et al.*, 2020). The shoulder band around 970 cm^{-1} can be attributed to B–O stretching vibrations in BO_4 units from tri– ($B_3O_5^-$), tetra– ($B_8O_{13}^{2-}$), and penta–borate ($B_5O_8^-$) groups (Varsamis *et al.*, 2000). The broad and strong band observed at ~1150 cm^{-1} is assigned to stretching vibrations of B–O bonds in BO_3 units from meta– and ortho–borate groups (Motka *et al.*, 2002), (Bhogi *et al.*, 2020). The shoulder band located ~1245 cm^{-1} is due to the asymmetric stretching vibration of the B–O bond of the triangle BO_3 unit containing non-bridging oxygen ions. The addition of Na_2O in the 78.5B_2O_3–21.5Bi_2O_3 glass matrix, gives a slight significant difference in the line shapes of this glass (**Figure 6**). Absorption bands of symmetric stretching vibrations of Bi–O bonds in pyramidal BiO_3 units shift from 700 cm^{-1} for x=0% to 698 com^{-1} for x=8% and its intensity decrease as the Na_2O content increases. In addition, it is observed that the band attributed to symmetric stretching vibrations of Bi–O bonds in BiO_3 units and stretching vibrations of B–O bonds in BO_4 units from di-borate group shift to lower frequencies progressively upon increasing Na_2O content. Absorption band at 1150 cm^{-1} assigned to stretching vibrations of B–O bonds in BO_3 units in bismuth borate disappear in the spectra of sodium doped bismuth borate glasses. The obtained spectra of selected glasses with x>0 show de presence of

absorption bands at 1360 cm^{-1} attributed to stretching vibrations of the B–O^{-} in pyroborate units, $BØO_2^{2-}$ (Ø bridging oxygen) (Dimitrov *et al.*, 1994), (Bhogi *et al.*, 2020), (Kamitsos *et al.*, 1990), (Winterstein-Beckmann *et al.*, 2015).

The bands shift to lower frequencies and the appearance of bands around 1360 cm^{-1} for glasses with x>0 may be attributed to the progressive depolymerization of the borate network as meta-borate triangles, $BØ_2O^-$, pyroborate dimers $B_2O_5^{4-}$, ortho-borate monomers BO_3^{3-}. The band at 1272 cm^{-1} in glass sample with x=0 has been found to be shifted at 1226 cm^{-1} for x=8%. These results can be explained by the continuous conversion of BO_3 trigonal units into BO_4 tetrahedral units as Na_2O is added. Previous studies of lithium borate (Moncke *et al.*, 2016) and silver borate (Kamitsos *et al.*, 1987) glasses, showed that replacement of a bridging oxygen (Ø) by a non−bridging one (O^-) in a $BØ_3$ triangle to form a $BØ_2O^-$ unit will reduce the symmetry. Similar results were found in recent studies of highly modified borate glasses (Winterstein-Beckmann *et al.*, 2013), (Lan *et al.*, 2021), (Singh *et al.*, 2014).

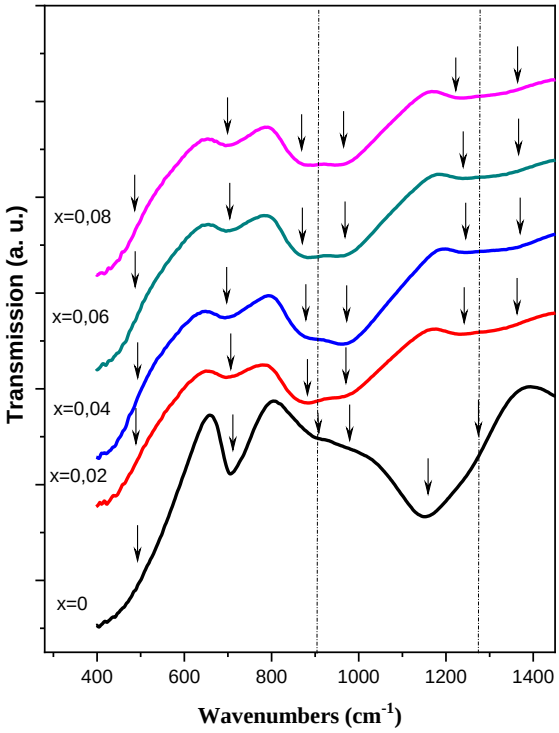

Figure 6. Infrared spectra of the (100–x)(0.785B_2O_3–0.215Bi_2O_3)–xNa_2O glasses

3.4.2. Raman spectroscopy

Raman scattering spectra of the studied glass samples (100–x)(0,785B_2O_3–0,215Bi_2O_3)–xNa_2O (0≤x≤8 mol.%), are recorded at room temperature in the frequency range 140–1400 cm^{-1} are shown in **Figure 7**. The main peak positions and vibration modes of Raman spectra are given in **Table 2**. Since more bands presented in **Figure 7** are broad and asymmetric, presenting some shoulders, and are an overlapping of some individual bands, a deconvolution of the obtained spectra was necessary. Raman spectrum of each sample is deconvoluted into distinct peaks by multiple peak fit modules of Origin Pro 8.6 software. Typical deconvoluted Raman spectra for glass samples with x = 0 and x=6 are shown in **Figure 8 a & b** respectively. The result of spectrum deconvolution indicates several peaks in the spectral region from 150 to 1400 cm^{-1}. **Figure 8 a** (x=0) shows the presence of peaks in the ranges: 153−156 cm^{-1}, 153−156 cm^{-1}, 175−204 cm^{-1}, 332−338 cm^{-1}, 410−441 cm^{-1}, 586−596 cm^{-1}, 1175−1200 cm^{-1} and 1280−1330 cm^{-1}. The peaks appearing at the positions ranging from 153

to 204 cm^{-1} can be due to the heavy metal Bi^{3+} vibrations in the BiO_3 pyramidal and BiO_6 octahedral units (Winterstein-Beckmann *et al.*, 2013), (Lan *et al.*, 2021), and to the vibrational modes of Bi—O in BiO_3 and BiO_6 units of the glass matrix (Singh *et al.*, 2014), (Baia *et al.*, 2002) (Subhadra *et al.*, 2012). The peaks between 332 cm^{-1} to 441 cm^{-1} can be considered as the vibrational modes of Bi–O–Bi band of the BiO_6 octahedral units (Singh *et al.*, 2014), (Baia *et al.*, 2002), (Subhadra *et al.*, 2012). The vibrational modes appeared from 586 to 596 cm^{-1} range, can be attributed to the vibrations occurring both due to the $Bi–O^-$ stretching in the BiO_6 units (Singh *et al.*, 2014), (Baia *et al.*, 2002), (Kaur *et al.*, 2018). The bands ranging from 1175 to 1200 cm^{-1} may be assigned to asymmetric stretching vibrations of terminal $B–O^-$ bonds of BO_3 units in pyro–borate group (Baia *et al.*, 2005), (Bala *et al.*, 2020). The peaks at the positions from 1281 to 1330 cm^{-1}, can be attributed to the vibrational response of stretching vibrations of $B–O^-$ bonds. The $B–O^-$ bonds comprise of pyroborate groups which are a part of connected boron–oxygen network. Many of the peaks at 900−1330 cm^{-1} range have been assigned to the vibrational modes due to the vibrations in the bonding B–O of the BO_3 and BO_4 units present in the network (Singh *et al.*, 2014), (Bala *et al.*, 2020), (Kaur *et al.*, 2018), (Ardelean *et al.*, 2008).

The addition of Na_2O to $78{,}5B_2O_3$–$21{,}5Bi_2O_3$ glass (x>0), results in the appearance of peaks ranging from 918 cm^{-1} to 1020 cm^{-1}. These peaks can be ascribed to the presence of vibrational modes occurring in the bonds like B–O–B and B–O present in the pyroborate and orthoborate groups of BO_3 triangular units (Winterstein-Beckmann *et al.*, 2013), (Lan *et al.*, 2021), (Ardelean *et al.*, 2008), (Bale *et al.*, 2008). On other hand, there was a split of the peak ranging from 1186 cm^{-1} to 1275 cm^{-1} in two peaks at 1180−1200 cm^{-1} and 1281−1330 cm^{-1} ranges, with an increase in the intensities of high frequencies peaks (**Figure 8 a & b**). Moreover, the obtained Raman spectra for all studied glass samples didn't exhibit peak at 800 cm^{-1} may support the absence of boroxol rings in the glass structure (Walrafen *et al.*, 1980).

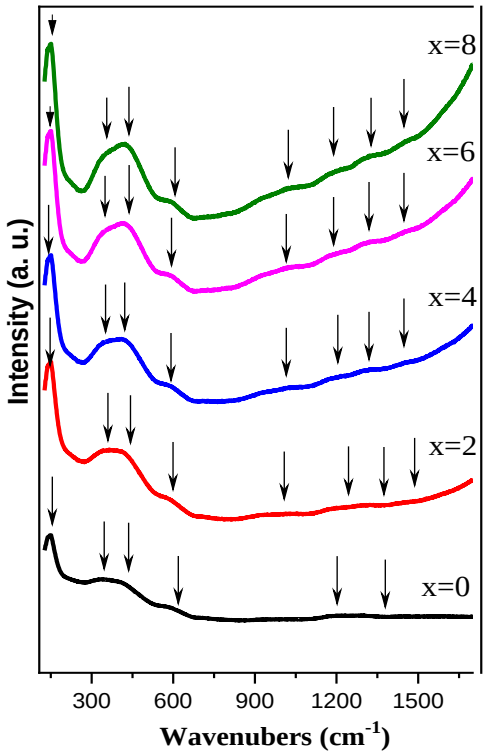

Figure 7. Raman spectra of the $(100–x)(0.785B_2O_3–0.215Bi_2O_3)–xNa_2O$ glasses

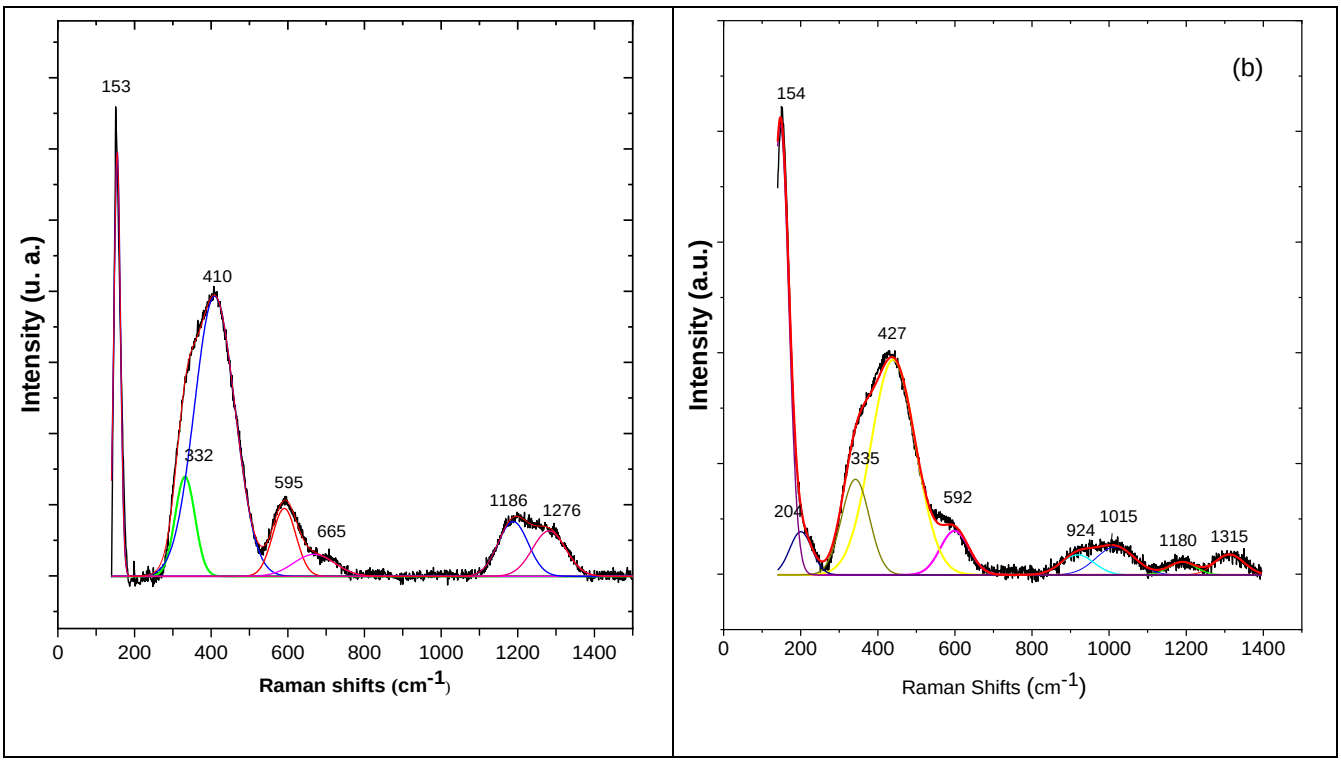

Figure 8. Deconvoluted Raman spectrum for: (a) $78.5B_2O_3$–$21.5Bi_2O_3$ (x=0) glass; (b) $73.79B_2O_3$–$20.21Bi_2O_3$–$6Na_2O$ (x=6) glass

Table 2. Observed IR band positions and Raman shifts and their assignments in $(100–x)(0.785B_2O_3–0.215Bi_2O_3)–xNa_2O$ glasses

IR bands (cm^{-1})	Raman shifts (cm^{-1})	IR assignments	Raman assignments
	153–204		Bi^{3+} cations are incorporated in BiO_3 and BiO_6 groups
440–450	332–441	Stretching vibrations of Bi–O bonds in strongly distorted vibrations BiO_6 units	
	586–596		Bi–O^- stretching vibrations of BiO_6 units
700–710		B–O–B bending vibrations in BO_3 triangles O_3B–O–BO_3 bending vibrations	
880–900		Symmetric stretching vibrations of Bi–O bonds in BiO_3 units, and stretching vibrations of B–O bonds in BO_4 units from diborate groups	
970–980	918–1020	Stretching vibrations of B–O bonds in BO_4 units from tri–, tetra– and pentaborate groups	B–O–B and B–O in pyroborate and orthoborate groups of BO_3 triangular units
1155–1240	1175−1200	B–O–B stretch in pyroborate units, $BØO_2^{2-}$ B–Ø stretch in $BØ_2O^-$ units	asymmetric stretching vibrations of terminal B–O^- bonds of BO_3 units in pyro–borate group
	1281−1330		$BØ_2O^-$ triangles linked to $BØ_4^-$ units
~1360		B–O^- stretch in pyroborate units, $BØO_2^{2-}$	

3.4.3. Structural model

The observed changes in the FTIR and Raman spectra of $(100-x)(0.785B_2O_3-0.215Bi_2O_3)$ $-xNa_2O$ ($0\leq x\leq 8$ mol.%) selected glasses, with the addition of sodium ions, suggest that the studied glasses reveal relatively less rigidity of the host glass matrix. The glassy network consists mainly of boron atoms as BO_3 and BO_4 units, while Bi^{3+} cations are incorporated into the network of these glasses as BiO_3 and BiO_6 units. It has been previously reported (Bhogi *et al.*, 2020), (Ciceo Lucacel *et al.*, 2007) that in borate glasses an isomerization occurs between the three and four coordinate boron entities, as $BO_3 \leftrightarrows BO_4$ (i). The observed increase of four−coordinated boron in the Raman and FTIR spectra with increasing Na_2O content can be expected from the right-shifting reaction (i) in the studied compositional range. This is attributed to the conversion of BO_3 to BO_4 structural units as the Na_2O glass modifier content increases, that is, the BO_3 units in bismuth borate $(0.785B_2O_3-0.215Bi_2O_3)$ glass prefer a coordination change from three to four over producing non−bridging oxygen (Ibrahim *et al.*, 2014), (Paşcuţă *et al.*, 2008).

Indeed, the basic structure of pure glassy B_2O_3, is known to be BO_3 groups bonded together to form a random network of boroxol rings, in addition to BO_3 triangles, connected by B–O–B (Krogh-Moe, 1965), (Umari *et al.*, 2005). The addition of Na_2O to the matrix, results in the progressive depolymerization of the borate network glasses, through the breaking of B–O–B linkages and the creation of non-bridging oxygen atoms (O^-). Thus, the short-range order $BO_{3/2}$ triangles are transformed initially to charged triangular borate units $BO_{2/2}O^-$, then by the isomerization process between BO_3 and BO_4 units, whereby the sp^2 planar units of $BO_{2/2}O^-$ are converted to the more stable sp^3 tetrahedral units of $BO_{4/2}^-$ (Krogh-Moe, 1962), (Mozzi *et al.*, 1970). The further increase content of Na_2O transform the boroxol rings into complex borate groups such as di-borate, penta-borate, metaborate, pyroborate, etc. (Lelong *et al.*, 2017), (Bodker *et al.*, 2019), (Ferlat *et al.*, 2008). The process can be represented as follows:

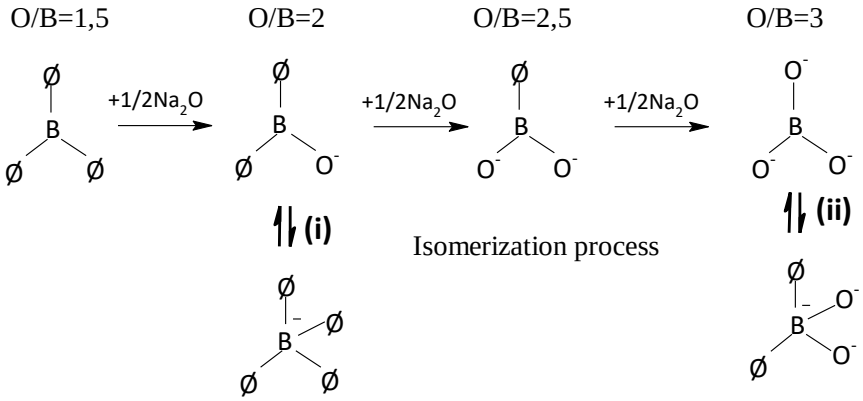

Conclusion

Sodium bismuth borate ternary glasses were prepared by melt quenching. The presence of a broad band in the X–ray diffraction patterns and the glass transition temperature (T_g) in the DSC curve are evidence of the glassy nature of all samples. The variation of the density, the molar volume, and the glass transition temperature with Na_2O content is related to the structural changes taking place in the glass. The addition of Na_2O to the glass matrix results in a decrease in the density of the glass, while the molar volume increases, leading to a less compact glass network. The FTIR and Raman spectroscopic studies performed on the selected samples concluded that there is a gradual conversion of trigonal BO_3 units to tetrahedral BO_4 units in the glass network with increasing amount of sodium oxide. Bi_2O_3 was found to exist as octahedral BiO_6 and pyramidal BiO_3 units in all glass networks.

Acknowledgments: The authors would like to thank M. Haddad of Moulay Ismail University, Faculty of Sciences, LASMAR - URAC 11, Meknes, Morocco, for her help in the measurements of Raman spectra.

References

Abid M., Belfaquir M., Hafid M., Taibi M., (2019) Study of zinc and lead addition effect on structure-properties of phosphate glasses, *Mater. Today: Proc.*, 13(part 3), 458–465. DOI:https://doi.org/10.1016/j.matpr.2019.04.002

Alaoui Y., El Moudane M., Er-rafai A., Khachani M., Ghanimi A., Sabbar A., Tabyaoui M., Guenbour A., Bellaouchou A., (2021) Structural study, thermal and physical properties of K_2O–CaO–P_2O_5 phosphate glasses, *Mor. J. Chem.* 9(3), 454–463. DOI: https://doi.org/10.48317/IMIST.PRSM/morjchem-v9i2.22505

Ardelean, I., & Cora, S. (2008). FT-IR, Raman and UV–VIS spectroscopic studies of copper doped $3Bi_2O_3 \cdot B_2O_3$ glass matix. *J. Mater. Sci.: Mater. Electron.*, 19, 584–588. DOI: https://doi.org/10.1007/s10854-007-9393-3

Baia L., Stefan R., Kiefer W., Popp J., Simon S., (2002) Structural investigations of copper doped B_2O_3–Bi_2O_3 glasses with high bismuth oxide content, *J. Non−Cryst. Solids* 303, 379–386. DOI:https://doi.org/10.1016/S0022-3093(02)01042-6

Baia L., Stefan R., Kiefer W., Simon S., (2005) Structural of characteristics of B2O3–Bi2O3 glasses with high transition metal oxide content, J. Raman Spectrosc. 36, 262–266. DOI: https://doi.org/10.1002/jrs.1306

Bajaj A., Khanna A., Chen B., Longstaffe J. G., Zwanziger U. W., Zwanziger J. W., González F., (2009) Structural investigation of bismuth borate glasses and crystalline phases, *J. Non−Cryst. Solids* 355, 45–53. DOI: https://doi.org/10.1016/j.jnoncrysol.2008.09.033

Bala M., Agrohiya S., Dahiya S., Ohlan A., Punia R., Maan A. S., (2020) Effect of replacement of Bi2O3 by Li_2O on structural, thermal, optical and other physical properties of zinc borate glasses, *J. Mol. Struct.* 1219, 128589. DOI: https://doi.org/10.1016/j.molstruc.2020.128589

Bale S., Rahman S., Awasthi A.M., Sathe V., (2008) Role of Bi_2O_3 content on physical, optical and vibrational studies in Bi_2O_3–ZnO–B_2O_3 glasses, *J. Alloys Compd.* 460, 699–703. DOI: https://doi.org/10.1016/j.jallcom.2007.06.090

Bengisu M., (2016) Borate Glasses for Scientific and Industrial Applications: A Review, *J. Mater. Sci.* 51, 2199–2242. DOI: https://doi.org/10.1007/s10853-015-9537-4

Bhogi A., , Pothuganti P. K. , Kistaiah P., (2020) Structural properties of Li_2O–BaO–B_2O_3–Fe_2O_3 glasses, *AIP Conf. Proc.* 2220, 080058–1–080058–6; DOI: https://doi.org/10.1063/5.0001158

Bodker M. S., Mauro J. C., Youngman R. E., Smedskjaer M. M., (2019) Statistical Mechanical Modeling of Borate Glass Structure and Topology: Prediction of Superstructural Units and Glass Transition Temperature, *J. Phys. Chem. B* 123, 1206–1213. DOI: https://doi.org/10.1021/acs.jpcb.8b11926

Bouhazma S., Chajri S., Barkai H., Elabed S., Ibnsouda Koraichi S., El Bali B., Lachkar M., (2015) Synthesis, characterization, in vitro bioactivity and wettability of sol–gel derived SiO_2–CaO–P_2O_5 and SiO_2–CaO–P_2O_5–Na_2O bioglasses, *Mor. J. Chem.* 3(1), 19–27. DOI: https://doi.org/10.48317/IMIST.PRSM/morjchem-v3i1.2257

Chourti K., Marchet P., Elhafiane Y., Bendahhou A., El barkany S., Karroua M., Abou-salama M., (2020) Relationships between crystalline structure and dielectric properties in $Sr_2Sm_{(1-x)}Nd_xTi_2Nb_3O_{15}$ ceramics, *Mor. J. Chem.* 8(1), 304–317. DOI: https://doi.org/10.48317/IMIST.PRSM/morjchem-v8i1.18479

Ciceo Lucacel R., Marcus C., Timar V., Ardelean I., (2007) FT-IR and Raman spectroscopic studies on B_2O_3–PbO–Ag_2O glasses dopped with manganese ions, *Solid State Sci*. 9, 850. DOI: https://doi.org/10.1016/j.solidstatesciences.2007.07.006

Dimitrov V., Dimitriev Y., Montenero A., (1994) IR spectra and structure of V_2O_5–GeO_2–Bi_2O_3 glasses, *J. Non–Cryst. Solids* 180, 51. DOI: https://doi.org/10.1016/0022-3093(94)90396-4

Doweidar H., (2014) Insights into the structure of Bi_2O_3–B_2O_3 glasses as predicted from density correlations, *J. Non−Cryst. Solids* 404, 49–54. DOI: https://doi.org/10.1016/j.jnoncrysol.2014.07.045
El-Hezzat M., Atbir A., Abid M., Montagne L., Méar F.O., (2021) Structure – Properties study of Na_2O–CaO–PbO–P_2O_5 metaphosphate glasses, *Solid State Sci.* 118, 106666.
DOI: https://doi.org/10.1016/j.solidstatesciences.2021.106666
Ersundu A. E., Elikbilek M. C, Aydin S., (2011) Characterization of B_2O_3 and/or WO_3 Containing Tellurite Glasses, *J. Non−Cryst. Solids* 358, 641–647. DOI: https://doi.org/10.1016/j.jnoncrysol.2011.11.012
Evidence of Mixed Alkali Effect", *J. Phys. Chem. A* 113, 2397–2404. DOI: https://doi.org/10.1021/jp809318e
Ferlat G., Charpentier T., Seitsonen A. P., Takada A., Lazzeri M., Cormier L., Calas G., Mauri F., (2008) Boroxol Rings in Liquid and Vitreous B_2O_3 from First Principles, *Phys. Rev. Lett.* 101, 65504. DOI: https://doi.org/10.1103/PhysRevLett.101.065504
Fuxi G., (1991) Optical and Spectroscopic Properties of Glass, *Springer, Berlin*.
Ibrahim S., Gomaa M. M., Darwish H., (2014) Influence of Fe_2O_3 on the physical, structural and electrical properties of sodium lead borate glasses, *J. Adv. Ceram.* 3 (2), 155–164. DOI: https://doi.org/10.1007/s40145-014-0107-z
Iordanova R., Dimitriev Y., Dimitrov V., Kassabov S., Klissurski D., (1996) Glass formation and structure in the V_2O_5–Bi_2O_3–Fe_2O_3 glasses, *J. Non−Cryst. Solids* 204, 141. DOI: https://doi.org/10.1016/S0022-3093(96)00416-4
Jabraoui H., Achhal E.M., Hasnaoui A., Garden J. L., Vaills Y., Ouaskit S., (2016) Molecular dynamics simulation of thermodynamic and structural properties of silicate glass: Effect of the alkali oxide modifiers, *J. Non−Cryst. Solids* 448, 16–26. DOI: https://doi.org/10.1016/j.jnoncrysol.2016.06.030
Kamitsos E. I., Patsis A. P., Karakassides M. A., Chryssikos G. D., (1990) Infrared reflectance spectra of lithium borate glasses, *J. Non−Cryst. Solids* 126, 52–67. DOI: https://doi.org/10.1016/0022-3093(90)91023-K
Kamitsos E.I., Karakassides M.A., Cryssikos G.D., (1987) Vibrational spectra of magnesium–sodium–borate glasses. 2. Raman and mid–infrared investigation of the network structure, *J. Phys. Chem.* 91, 1073. DOI: https://doi.org/10.1021/j100289a014
Kaur P., Singh K.J., Thakur S., Singh P., Bajwa B. S., (2018) Investigation of bismuth borates glass system modified with barium for structural and gamma-ray shielding properties, *Acta Part A* 206, 367–377. DOI: https://doi.org/10.1016/j.saa.2018.08.038
Krogh-Moe J., (1962) The crystal structure of lithium diborate, Li_2O. $2B_2O_3$, *Phys. Chem. Glasses* 3, 101, 16. DOI: https://doi.org/10.1107/S0365110X6200050X
Krogh-Moe J., (1965) Interpretation of infrared spectra of boron oxide and alkali borate glasses, *Phys. Chem. Glasses* 6, 46.
Lan, S. H., Lee, C. T., Lai, Y. S., Chen, C. C., & Yang, H. W. (2021). The relationship between the structure and thermal properties of Bi_2O_3–ZnO–B_2O_3 glass system. *Adv. Condens. Matter Phys.*, 2021, 1-12. DOI: https://doi.org/10.1155/2021/2321558
Lelong G., Cormier L., Hennet L., Michel F., Rueff J. P., Ablett J. M., Monaco G., (2017) Lithium borate crystals and glasses: how similar are they? A non-resonant inelastic X-ray scattering study around the B and O Kedges, *J. Non−Cryst. Solids* 472, 1–8. DOI: https://doi.org/10.1016/j.jnoncrysol.2017.06.012
Minakova N., Zaichuk A., Belyi Y., (2008) The Structure of Borate Glass, *Glass and Ceram.* 65, 70–73.
Moncke D., Kamitsos E. I., Palles D., Limbach R., Winterstein-Beckmann A., Honma T., Yao Z., Rouxel T., Wondraczek L., (2016) Transition and post–transition metal ions in borate glasses: borate ligand speciation, cluster formation and their effect on glass transition and mechanical properties, *J. Chem. Phys.* 145, 124501. DOI: https://doi.org/10.1007/s10717-008-9017-2
Motke S.G., Yawale S.P., Yawale S.S., (2002) Infrared spectra of zinc doped lead borate glasses, *Bull. Mater. Sci.* 25, 75. DOI: https://doi.org/10.1007/BF02704599
Mozzi R. L., Waren B. E., (1970) The structure of vitreous boron oxide, *J. Appl. Crystallogr.* 3(4), 251−257. DOI: https://doi.org/10.1107/S0021889870006143

Paşcuţă P., Boşca M., Rada S., Culea M., Bratu I., Culea E., (2008) FTIR spectroscopic study of Gd_2O_3–Bi_2O_3–B_2O_3 glasses, *J. Optoelectron. Adv. M.* 10(9), 2416–2419. DOI: https://doi.org/10.1007/s10854-008-9734-x

Rajyasree Ch., Krishna Rao D., (2011) Spectroscopic investigations on alkali earth bismuth borate glasses doped with CuO, *J. Non−Cryst. Solids* 357, 836–41. DOI: https://doi.org/10.1016/j.jnoncrysol.2010.11.008

Sanghi S., Pal I., Agarwal A., Aggarwal M. P., (2011) Effect of Bi_2O_3 on spectroscopic and structural properties of Er^{3+} doped cadmium bismuth borate glasses, *Spectrochim. Acta A Mol. Biomol. Spectrosc.* 83(1), 94–99. DOI: https://doi.org/10.1016/j.saa.2011.07.084

Shaaban R. E., Shapaan M., Saddeek Y. B., (2008) Structural and thermal stability criteria of Bi_2O_3–B_2O_3 glasses, *J. Phys. Condens. Matter* 20, 155108. DOI: https://doi.org/10.1088/0953-8984/20/15/155108

Shaim A., Et−Tabirou M., Montagne L., Palavit G., (2002) Role of bismuth and titanium in Na_2O–Bi_2O_3–TiO_2–P_2O_5 glasses and a model of structural units, *Mater. Res. Bull.* 37, 2459. DOI: https://doi.org/10.1016/S0025-5408(02)00929-7

Sharma G., Singh K., Manupriya, Mohan S., Singh H., Bindra S., (2006) Effects of gamma irradiation on optical and structural properties of PbO–Bi_2O_3–B_2O_3 glasses, *Radiat. Phys. Chem.* 75 (9), 959–966. DOI: https://doi.org/10.1016/j.radphyschem.2006.02.008

Singh L., Thakur V., Punia R., Kundu R.S., Singh A., (2014) Structural and optical properties of barium titanate modified bismuth borate glasses, Solid State Sci. 37, 64–71. DOI: https://doi.org/10.1016/j.solidstatesciences.2014.08.010

Subhadra M., Kistaiah P., (2012) Infrared and Raman spectroscopic studies on alkali borate glasses: evidence of mixed alkali effect, Vib. Spect. 62, 23–27. DOI: https://doi.org/10.1021/jp809318e

Suzuya K., Price D. L., Loong C. K., Martin S. W., (1998) Structure of vitreous P_2O_5 and alkali phosphate glasses, *J. Non−Cryst.* Solids 232–234, 650–657. DOI: https://doi.org/10.1016/S0022-3093(98)00529-8

Umari P., Pasquarello A., (2005) Fraction of Boroxol Rings in Vitreous Boron Oxide from a First-Principles Analysis of Raman and NMR Spectra, *Phys. Rev. Lett.* 95, 137401. DOI: https://doi.org/10.1103/PhysRevLett.95.137401

Varsamis C.P., Kamitsos E.I., Chryssikos G.D., (2000) Spectroscopic investigation of AgI–doped borate glasses, *Solid State Ionics* 136–137, 1031–1039. DOI: https://doi.org/10.1039/D1CP00301A

Walrafen G.E., Samanta S. R., Krishnan P.N., (1980) Raman investigation of vitreous and molten boric oxide, *J. Chem. Phys.* 72, 113–120. DOI: https://doi.org/10.1063/1.438894

Winterstein-Beckmann A., Moncke D., Palles D., Kamitsos E. I., Wondraczek L., (2015) Structure and Properties of Orthoborate Glasses in the Eu_2O_3−(Sr,Eu)O−B_2O_3 Quaternary, *J. Phys. Chem. B* 119, 3259–3272. DOI: https://doi.org/10.1021/jp5120465

Winterstein-Beckmann A., Moncke D., Palles D., Kamitsos E. I., Wondraczek L., (2013) Structure–property correlations in highly modified Sr, Mn–borate glasses, *J. Non−Cryst. Solids* 376, 165–174. DOI: https://doi.org/10.1016/j.jnoncrysol.2013.05.029

(2023) ; https://revues.imist.ma/index.php/morjchem/index